*Inorg. Chem.* **2009**, *48*, 4044−4051

# Magnetic Properties and Vapochromic Reversible Guest-Induced Transformation in a Bispyrazolato Copper(II) Polymer: an Experimental and Dispersion-Corrected Density Functional Theory Study

**Alessandro Bencini,[†] Maurizio Casarin,[‡,§] Daniel Forrer,[‡] Lorenzo Franco,[‡] Federica Garau,[‡] Norberto Masciocchi,[||] Luciano Pandolfo,[*,‡] Claudio Pettinari,[⊥] Marco Ruzzi,[‡] and Andrea Vittadini[*,‡,§]**

*Dipartimento di Chimica, Università di Firenze, via della Lastruccia 3, I-50019 Firenze, Italy, Dipartimento di Scienze Chimiche, Università di Padova, via Marzolo 1, I-35131 Padova, Italy, Istituto di Scienze e Tecnologie Molecolari del CNR (ISTM-CNR), via Marzolo 1, I-35131 Padova, Italy, Dipartimento di Scienze Chimiche e Ambientali, Università dell'Insubria, via Valleggio 11, I-22100 Como, Italy, and Dipartimento di Scienze Chimiche, Università di Camerino, via S.Agostino 1, I-62032 Camerino(MC), Italy*

Received October 10, 2008

Dispersion-corrected density functional theory (DFT-D) calculations, Electron Spin Resonance spectroscopy (EPR), and variable temperature magnetic moment measurements were used to investigate the structure and the electronic/magnetic properties of bispyrazolato-copper(II) coordination polymer and of its hydration product. The Cu(II) ions are antiferromagnetically coupled through the $\sigma$ system of the pyrazolate rings in both compounds. Theoretical electron density maps reveal that water molecules interact simultaneously and to a comparable extent with two Cu(II) centers (through the electronegative O end) and two pyrazolate rings (through the partly positively charged H atoms), which is compatible with the observed internuclear distances. DFT-D calculations indicate that low kinetic barriers are involved in the rearrangement of the host structure.

## Introduction

The increasing demand for better materials for gas sensing and gas storage applications has stimulated the design of new porous materials based on molecular frameworks. This crystal engineering process is, however, hampered by the natural tendency of molecular systems to pack as close as possible, intrinsically limiting the number of porous compounds.[1] In this context, a promising class of materials is represented by systems which are able to reversibly change their crystal structure in the presence of guest molecules in such a way as to create otherwise absent pores or to modify their shapes, dimensions, and/or functional properties.[2]

In a recent communication,[2a] some of us reported on the synthesis of a novel polymorph (the "$\beta$" phase) of copper(II) pyrazolate, $\beta$-$[Cu(pz)_2]_n$, a one-dimensional (1D) coordination polymer obtained by reacting Cu(II) carboxylates with pyrazole (Hpz) in MeCN. Remarkably, this compound is able, in the solid state, to absorb/desorb water and several other small guest molecules (viz. $NH_3$, $MeNH_2$, $CH_3CN$, pyridine, MeOH, and EtOH) through a reversible change of the mutual arrangement of the polymer chains, accompanied by significant color modifications. The crystal structure of the anhydrous and of the hydrated polymers were determined by X-ray powder diffraction (XRPD) methods: $\beta$-$[Cu(pz)_2]_n$, crystallizes in the monoclinic system ($P2_1/m$ space group; $a$ = 9.055 Å, $b$ = 7.401 Å, $c$ = 5.597 Å, $\beta$ = 99.48°, see Figure 1a), whereas the hydrated phase $[Cu(pz)_2 \cdot (H_2O)]_n$, is orthorhombic (*Cmcm* space group; $a$ = 16.960 Å, $b$ = 6.236 Å, $c$ = 7.283 Å, see Figure 1c).

In our preliminary communication,[2a] the presence of a magnetic interaction coupling the Cu(II) ions was noted. In this work, we address in more detail these magnetic interactions from an experimental and computational point of view, and we obtain more detailed information on the bonding between the host and the guest water molecules, for which an approximate location was experimentally

* To whom correspondence should be addressed. E-mail: andrea.vittadini@unipd.it.
[†] Università di Firenze.
[‡] Università di Padova.
[§] Istituto di Scienze e Tecnologie Molecolari del CNR.
[||] Università dell'Insubria.
[⊥] Università di Camerino.



10.1021/ic801928b CCC: $40.75 
Published on Web 04/06/2009

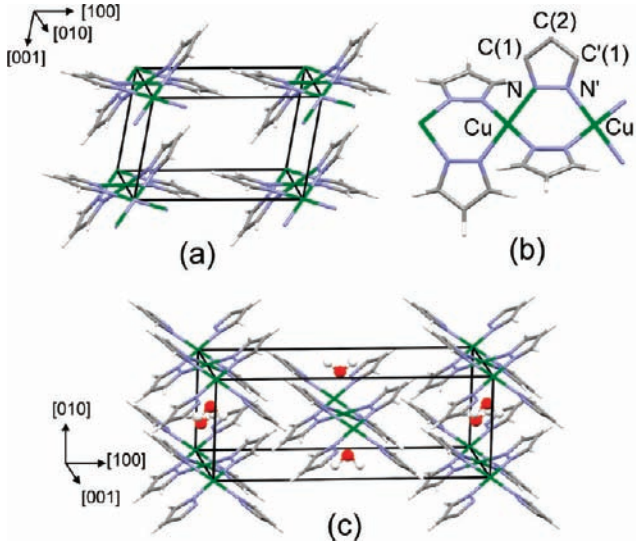


**Figure 1.** (a) Schematic drawings of: (a) $\beta$-$[Cu(pz)_2]_n$; (b) a portion of the $Cu(pz)_2$ chain running along [010]; (c) the unit cell of $[Cu(pz)_2 \cdot (H_2O)]_n$. The $H_2O$ molecules, shown in a ball-and-stick representation, are in the equilibrium configuration as determined by the DFT calculations.

determined by XRPD. Furthermore, we investigate the mechanism of the structure transformations involved in the water sorption/desorption processes. Finally, we report also a new and more efficient synthetic procedure for the obtaining of $\beta$-$[Cu(pz)_2]_n$, that has also made possible its embedding into pumice sheets.

## Material and Methods

**Synthesis and Sample Manipulation.** If not otherwise stated, reactions and manipulations were carried out in the air. Reagents (Aldrich) were used without further purification. Elemental analyses (C, H, N) were performed with a Fisons Instruments 1108 CHNS-O Elemental Analyzer. IR spectra were recorded from 4000 to 400 $cm^{-1}$ with a Perkin-Elmer 983 instrument. UV−vis spectra were recorded from 200 to 800 nm with a Varian Cary 5E instrument.

$[Cu(pz)_2 \cdot (NH_3)]_n$, **1**.

This species was obtained by slightly modifying a procedure reported by Inoue et al.[3]

A solution of $Cu(NO_3)_2 \cdot 2.5H_2O$ (1.823 g, 7.83 mmol) in 40 mL of 28% aqueous ammonia was added at room temperature (r.t.) under vigorous stirring to a solution of 1.088 g of Hpz (15.98 mmol) in 40 mL of 28% aqueous ammonia. The obtained dark-blue suspension was stirred for 20 min obtaining a blue precipitate that was filtered, washed with 28% aqueous ammonia, and dried under vacuum (0.1 mmHg) at r.t., obtaining 1.31 g of a blue solid (Yield 78%). Similar results were obtained by using copper(II) sulfate and copper(II) chloride.

**1**. Elem. Anal. Calcd for $C_6H_9N_5Cu$: C, 33.56; H, 4.22; N, 32.62. Found: C, 33.98; H, 3.91; N, 31.99.

Mp. At about 120 °C compound **1** turns into a light-brown solid ($\beta$-$[Cu(pz)_2]_n$, **2**, vide infra), stable up to about 300 °C, where decomposition begins.

$\beta$-$[Cu(pz)_2]_n$, **2**.

$[Cu(pz)_2 \cdot (NH_3)]_n$, **1**, (266.8 mg, 1.24 mmol) was heated (90 °C) under dynamic vacuum (0.1 mmHg) for 15 min observing a weight loss of 20.9 mg, corresponding to the elimination of 1.23 mmol of $NH_3$, and the simultaneous color change into beige.

**2**. Elem. Anal. Calcd for $C_6H_6N_4Cu$: C, 36.45; H, 3.06; N, 28.34. Found: C, 36.09; H, 3.30; N, 28.25.

$[Cu(pz)_2 \cdot (H_2O)]_n$, **3**.

Compound **2** at 25 °C easily absorbs water vapors from the air or from solvate moist environments and rapidly yields the pale-pink derivative $[Cu(pz)_2 \cdot (H_2O)]_n$, **3**.

**3**. Elem. Anal. Calcd for $C_6H_8N_4OCu$: C, 33.41; H, 3.74; N, 25.97. Found: C, 33.12; H, 3.85; N, 25.67.

The identity of **1**, **2**, and **3** was confirmed by their IR, UV−vis, and XRPD spectra that resulted identical to those previously reported.[2a] Moreover, **2** adsorbs reversibly $NH_3$, $H_2O$, $MeNH_2$, and so forth, yielding the corresponding solvated derivatives previously reported.[2a] Cycles of sorption/desorption of water and $NH_3$ were repeated on compound **2** 10 times without observing any degradation.

**Embedding of 1, 2, and 3 into Pumice Sheets.** Sheets of pumice (ca. 10 × 20 × 1 mm) were obtained by cutting a commercial pumice block obtained from a local hardware store. Subsequently. the sheets were accurately washed with water, maintained in *aqua regia* for 1 h, washed with running tap water for 2 h, with running deionized water for 1 h, put into 28% $NH_3$ aqueous solution for 2 h, rinsed with running deionized water for 20 min, and then dried by vacuum pumping (0.1 mmHg) for 8 h at r.t. The cleaned sheets of pumice were soaked for 2 h into a solution of Hpz (0.388 g, 5.7 mmol) in a 28% $NH_3$ aqueous solution and then dipped into a stirred solution of $Cu(NO_3)_2 \cdot 2.5H_2O$ (0.676 g, 2.9 mmol) in 10 mL of 28% $NH_3$ aqueous solution and here maintained overnight. Deep-blue colored sheets formed, which were washed with running deionized water for 20 min and finally dried under vacuum (0.1 mmHg) at rt, the blue color being practically unchanged. Upon heating (ca. 90 °C) under dynamic vacuum (0.1 mmHg) for 20 min, the blue sheets turned beige, indicating that the transformation of embedded **1** in **2** occurred. Moreover the beige sheets, changed color (pale pink) when put in contact with $H_2O$ vapors (indicating the formation of embedded **3**) and became blue in the presence of $NH_3$, reversibly forming **1**, analogously to what was previously reported for pure bulk species.[2a] The sorption/desorption cycles of water and $NH_3$ were repeated 10 times also on these sheets, obtaining analogous results with respect to pure compounds.

**Electron Paramagnetic Resonance (EPR) Measurements.** The EPR spectra were recorded on about 10 mg of powdered samples put into 4 mm diameter quartz tubes, using a Bruker ER200D X-band spectrometer equipped with a nitrogen-flow variable temperature system for measurements in the temperature range 100−400 K. Typical acquisition parameters were: microwave power 10 mW, modulation amplitude 5 G, sweep time 3 min. For g-factor determination, the microwave frequency was measured using a HP5342 frequency counter, and the magnetic field was calibrated using a DPPH standard.

**Magnetic Susceptibility Measurements.** The temperature dependence of the magnetic susceptibility of all the compounds was measured using a Cryogenic S600 SQUID magnetometer. The measurements were performed on polycrystalline powder samples

(1) Barbour, L. J. *Chem. Commun.* **2006**, 1163.
(2) (a) Cingolani, A.; Galli, S.; Masciocchi, N.; Pandolfo, L.; Pettinari, C.; Sironi, A. *J. Am. Chem. Soc.* **2005**, *127*, 6144. (b) Yamada, K.; Tanaka, H.; Yagishita, S.; Adachi, K.; Uemura, T.; Kitagawa, S.; Kawata, S. *Inorg. Chem.* **2006**, *45*, 4322. (c) Takamizawa, S.; Kojima, K.; Akatsuka, T. *Inorg. Chem.* **2006**, *45*, 4580. (d) Supriya, S.; Das, S. K. *J. Am. Chem. Soc.* **2007**, *129*, 3464. (e) Dobrzan′ska, L.; Gareth, O.; Lloyd, G. O.; Esterhuysen, C.; Barbour, L. J. *Angew. Chem., Int. Ed.* **2006**, *45*, 5856. (f) Nagarathinam, M.; Vittal, J. J. *Angew. Chem., Int. Ed.* **2006**, *45*, 4337. (g) Serre, C.; Millange, F.; Thouvenot, C.; Noguès, M.; Marsolier, G.; Louer, D.; Férey, G. *J. Am. Chem. Soc.* **2002**, *124*, 13519. (h) Serre, C.; Mellot-Draznieks, C.; Surblé, S.; Audebrand, N.; Filinchuk, Y.; Férey, G. *Science* **2007**, *315*, 1828.
(3) Inoue, M.; Kishita, M.; Kubo, M. *Inorg. Chem.* **1965**, *4*, 626.

in an external magnetic field of 0.1 T varying the temperature between 2 and 300 K. $\beta$-$[Cu(pz)_2]_n$ was kept in an oven at 80 °C under vacuum for 24 h and weighed in a glovebox. All the data were corrected for diamagnetism.[4]

**Density Functional Calculations.** Density functional (DF) calculations were performed using the Perdew−Burke−Ernzerhof exchange-correlation functional[5] and Vanderbilt[6] pseudopotentials. Because the polymer chains interact through dispersion forces, the dispersion-corrected DFT-D method by Grimme,[7] recently implemented by some of us[8] in the Quantum-ESPRESSO package,[9] was adopted. A total of 11, 6, 5, 4, and 1 valence electrons were explicitly considered for Cu, O, N, C, and H, respectively. The smooth part of the wave function was expanded in plane waves, with a kinetic energy cutoff of 30 Ry, while the cutoff for the augmented electron density charge was 250 Ry. Plane wave calculations have been shown to be adequate for describing magnetic interactions in Cu(II) complexes.[10] The Brillouin zone integration was performed using the Monkhorst−Pack scheme,[11] with $2 \times 4 \times 2$ and a $1 \times 2 \times 4$ meshes for $\beta$-$[Cu(pz)_2]_n$, **2** and $[Cu(pz)_2 \cdot (H_2O)]_n$, **3**, respectively. Both lattice constants and internal parameters were fully optimized with a BFGS algorithm. Finite-basis set effects were corrected following the procedure by Bernasconi et al.[12] with $A = 40$ Ry, $E_0 = 30$ Ry, and $\sigma = 4$ Ry. Calculations were performed for both the ferromagnetic (FM) and the antiferromagnetic (AFM) states. The energy difference was used to estimate the exchange coupling $J$ by fitting to an Ising model.

## Results and Discussion

In 1965 Inoue et al.[3] in a study on the magnetic properties of a variety of copper(II) complexes with nitrogen heterocyclic ligands reported, inter alia, obtaining purple microcrystals of "bis(pyrazolato)copper(II) hemiammonia hemihydrate, $Cu(C_3H_3N_2)_2 \cdot 0.5NH_3 \cdot 0.5H_2O$" by reacting copper(II) sulfate with pyrazole in concentrated aqueous ammonia. They also observed that, on heating, the compound eliminated ammonia and water and the purple microcrystals turned brown, but this latter compound was not characterized further. Recently, we reported the synthesis and characterization of the $\beta$ polymorph, $\beta$-$[Cu(pz)_2]_n$, **2**,[2a] which is pale-brown and changes color on sorption of water and ammonia, giving $[Cu(pz)_2 \cdot (H_2O)]_n$, **3**, (pale pink) and $[Cu(pz)_2 \cdot (NH_3)]_n$, **1**, (blue), respectively. Suspecting that the brown compound observed by Inoue et al.[3] was **2**, we repeated their procedures in slightly different conditions (see Materials and Methods section) and succeeded in obtaining $[Cu(pz)_2 \cdot (NH_3)]_n$, **1**, in about 78% yield, somewhat lower with respect to the almost quantitative yield of our previous synthesis.[2a] On the other hand, this drawback is balanced by the possibility to use

**Scheme 1**

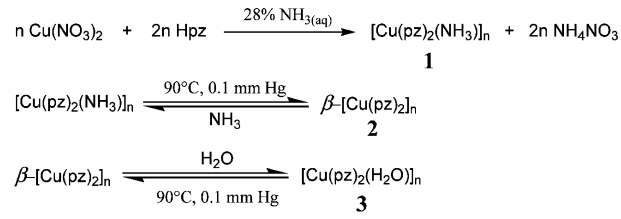


practically any copper(II) salt, and not only the more expensive carboxylates and, most important, to avoid the use of the organic solvents like MeCN. In this procedure MeCN is replaced by aqueous concentrated ammonia that acts also as deprotonating agent of Hpz, a role originally played by the carboxylate ions.[2a] Thus, the deprotonated pyrazoles coordinated to cuproammoniacal species formed by Cu(II) salts are dissolved in aqueous ammonia yielding **1**. The accessibility of the cavities and the diffusion of the reactants within the pores of the bulk pumice make it possible to prepare solid, resistant sheets where **1** is permanently adsorbed.

Pure crystalline powders of **1** or even **1** adsorbed into pumice sheets show the reversible sorption/desorption behavior discussed in ref 2a, and schematically sumarized in Scheme 1. This can be easily appreciated from Figure 2, where the different materials are collectively shown. This demonstrates that when suitably supported, the polymer could be in principle used to detect water or other small molecules.

**Magnetic Susceptibilty Results.** The temperature dependence of $\chi$ of **2** and **3** is typical of an antiferromagnetic linear chain of $S = 1/2$ spins[13,14] containing low amounts of paramagnetic impurities (Figure 3). Although much theoretical work has been done on low-dimensional magnetic systems in the last decades, there is still no exact closed-form equation for the temperature dependence of the magnetic susceptibility of a regular 1D chain of 1/2 spins described by the Heisenberg isotropic exchange Hamiltonian, $H = -J\sum_i \mathbf{S}_i \cdot \mathbf{S}_{i+1}$ ($J$ is the isotropic exchange coupling constants), which are valid for the whole temperature range. The magnetic susceptibility of these systems was originally solved by Bonner and Fisher,[13,15] who computed the magnetic susceptibilities of ring chains of increasing size (up to 11 magnetic centers), and proposed an extrapolation for the infinite ring. Close equations exist for the low temperature limit[15] when $J < 0$ (antiferromagnetic interaction), and for the high temperature region for both positive and negative $J$.[16] An efficient way of measuring $J$ is to use equations derived by fitting Bonner−Fisher's numerical

(4) O'Connor, C. J. *Prog. Inorg. Chem.* **1982**, *29*, 203.
(5) Perdew, J. P.; Burke, K.; Ernzerhof, M. *Phys. Rev. Lett.* **1996**, *77*, 3865.
(6) Vanderbilt, D. *Phys. Rev. B* **1990**, *41*, 7892.
(7) Grimme, S. *J. Comput. Chem.* **2006**, *27*, 1787.
(8) Barone, V.; Casarin, M.; Forrer, D.; Pavone, M.; Sambi, M.; Vittadini, A. *J. Comput. Chem.* **2009**, *30*, 934.
(9) Baroni, S.; dal Corso, A.; de Gironcoli, S.; Giannozzi, P.; Cavazzoni, C.; Ballabio, G.; Scandolo, S.; Chiarotti, G.; Focher, P.; Pasquarello, A.; Laasonen, K.; Trave, A.; Car, R.; Marzari, N.; Kokalj, A. http://www.pwscf.org.
(10) Massobrio, C.; Ruiz, E. *Monatsh. Chem.* **2003**, *134*, 317.
(11) Monkhorst, H.; Pack, J. *Phys. Rev. B* **1976**, *13*, 5188.
(12) Bernasconi, M.; Chiarotti, G. L.; Focher, P.; Scandolo, S.; Tosatti, E.; Parrinello, M. *J. Phys. Chem. Solids* **1995**, *56*, 501.
(13) Kahn, O. *Molecular Magnetism*; VCH Publishers: New York, 1993.
(14) Jotham, R. W. *J. Chem. Soc., Dalton Trans.* **1977**, 266.
(15) Bonner, J. C.; Fisher, M. E. *Phys. Rev. A* **1964**, *135*, 640.
(16) (a) Baker, G. A.; Rushbrooke, G. S.; Gilbert, H. E. *Phys. Rev.* **1964**, *135*, A1272. (b) Baker, G. A.; Rushbrooke, G. S.; Gilbert, H. E. *Phys. Rev.* **1967**, *164*, 800.

**Figure 2.** Pumice sheets embedding anhydrous $\beta$-$[Cu(pz)_2]_n$, **2**, (left), hydrated $[Cu(pz)_2 \cdot (H_2O)]_n$, **3**, (center), and ammonia complex $[Cu(pz)_2 \cdot (NH_3)]_n$, **1**, (right) together with corresponding microcrystalline powdered compounds.

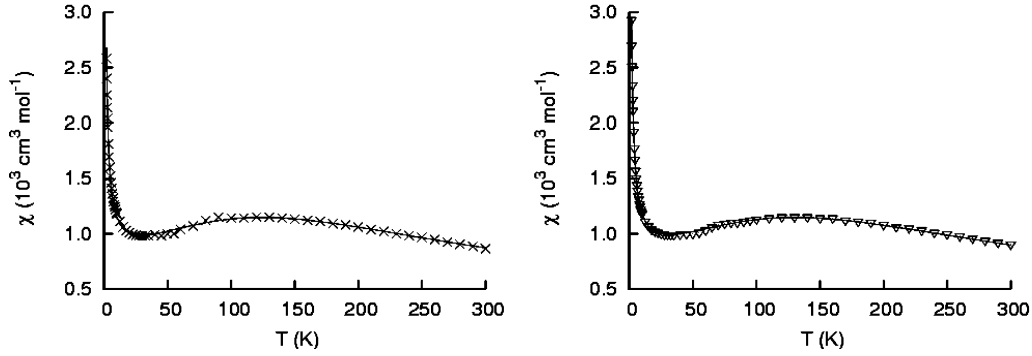


**Figure 3.** Temperature dependence of $\chi$ for $[Cu(pz)_2]_n$ (left) and $[Cu(pz)_2 \cdot (H_2O)]_n$ (right). Solid lines are the best fit curves (see text).

results with polynomial expressions by Jotham[14,15] and Hall.[17]

We used here the Hall equation:

$$\chi_{BF}(T) = \frac{Ng^2\mu_B^2}{kT}\frac{0.25 + 0.074975x + 0.075235x^2}{1.0 + 0.9931x + 0.172135x^2 + 0.757825x^3} \quad (1)$$

where $x = |J|/kT$.

Including in eq 1 the effect of a paramagnetic impurity, we obtain the working equation expressing the magnetic susceptibility, $\chi_c$, to be compared with the experimental values:

$$\chi_c(T) = \chi_{BF}(T)(1 - \rho) + \frac{Ng^2\mu_B^2}{3kT}\rho \quad (2)$$

where $\rho$ is the molar fraction of the impurity assumed to have the same $g$ of the Cu(II) ions in the chain. The magnetic data, $\chi_o(T_i)$, were fit using the MINUIT[18] routine keeping $J$ and $\rho$ as free parameters. Since $g$ and $J$ were found to be strongly correlated, $g$ was kept fixed at 2.07 (the value obtained from EPR spectra, vide infra). The experimental results are compared to the computed ones in Figure 3. The best fit curve (solid lines) were obtained with the parameters $J = -141.8(7)$ cm$^{-1}$, $\rho = 0.91(7)\%$ for $\beta$-$[Cu(pz)_2]_n$ and $J = -145.5(3)$ cm$^{-1}$, $\rho = 0.97(6)\%$ for $[Cu(pz)_2 \cdot (H_2O)]_n$. The agreement factors were $R = 1.5\%$ and $R = 0.5\%$ in the two cases, respectively.

Antiferromagnetic interactions are commonly observed in bis-pirazolato bridged dimers. Originally we reported a "weak exchange interaction" on the basis of preliminary results. On repeating and better analysing the experiments, more accurate values of $J$ (reported above) were determined, which can be considered rather high and in the range usually observed in dinuclear copper(II) complexes,[19] and compare well with those of the $\alpha$-$[Cu(pz)_2]_n$ phase ($J = -156$ cm$^{-1}$).[16,20] Unexpectedly, these values indicate a scarce sensitivity on the stereochemical parameters. As a matter of fact, magneto-structural correlations, within the orbital model of the exchange interactions, showed that deviation from co-planarity of the two pyrazolato ligands could affect even the sign of the exchange coupling constant, apparently counter balanced by the non-co-planarity of the Cu(II) coordination planes.[20,21]

**EPR Results.** EPR spectra of both $\beta$-$[Cu(pz)_2]_n$, **2**, and the hydrated compound $[Cu(pz)_2 \cdot (H_2O)]_n$, **3** at r.t., show a single isotropic resonance at $g = 2.07 \pm 0.01$. As a representative example, the polycrystalline EPR powder spectrum of $\beta$-$[Cu(pz)_2]_n$ is shown in Figure 4. The line shape is almost purely Lorentzian and the peak-to-peak line width is 230 G for **2** and 250 G for **3**.

The Lorentzian line shape, maintained throughout the investigated temperature range (100−350 K), is due to the relatively strong spin exchange interaction between copper atoms, which averages out all the anisotropies from the $g$-factor and hyperfine interactions. Likely, this occurs because magnetic exchange overcomes other relaxation mechanisms, like spin−lattice relaxation.[22] In the temperature

(17) (a) Hall, J. W. Ph.D. Dissertation, University of North Carolina, 1977. (b) Estes, W. E.; Gavel, D. P.; Hatfield, W. E.; Hodgson, D. *Inorg. Chem.* **1978**, *17*, 1415. (c) Estes, W. E.; Hatfield, W. E.; van Ooijen, J. A. C.; Reedijk, J. *J. Chem. Soc., Dalton Trans.* **1980**, 2121.
(18) James, F. *MINUIT*, version 96.03; CERN program library: Geneva.
(19) Tanase, S.; Koval, I. A.; Bouwman, E.; de Gelder, R.; Reedijk, J. *Inorg. Chem.* **2005**, *44*, 7860.
(20) Ehlert, M. K.; Retting, S. J.; Storr, A.; Thompson, R. C.; Trotter, J. *Can. J. Chem.* **1989**, *67*, 1970.
(21) Ajò, D.; Bencini, A.; Mani, F. *Inorg. Chem.* **1988**, *27*, 2437.

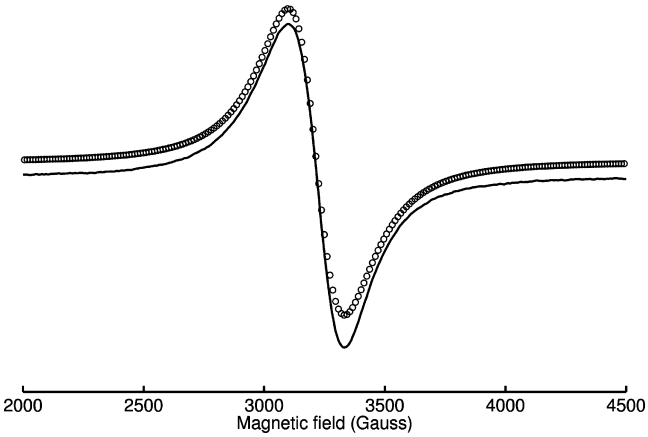


**Figure 4.** Room temperature polycrystalline powder EPR spectrum of $\beta$-$[Cu(pz)_2]_n$. Solid line: experimental spectrum. Circles: best fit Lorentzian line.

range 100−350 K, the doubly integrated EPR intensities show a maximum at about 160 K for **2** and at slightly higher temperature for **3** (data not shown).

The intensity of an EPR spectrum, when exchange interactions are dominating the relaxation mechanisms, is proportional to the magnetic susceptibility of the sample.[19] Therefore an estimate of $J$ can be obtained by fitting the EPR intensities with the polynomial expression of eq 2. The best fit values are $J = -168$ cm$^{-1}$ for **2** and $-190$ cm$^{-1}$ for **3**. Considering the larger uncertainties of the EPR results, these values are in fair agreement with magnetic susceptibility data.

Summarizing, magnetism and EPR measurements indicate that the presence of water molecules in the hydrated polymer is slightly increasing the superexchange interaction between the copper ions. This effect is, however, weak as a consequence of the relatively long Cu−$OH_2$ distance (as discussed below).

**Theoretical Calculations.** We first point out that this is, to our knowledge, the first application of the DFT-D method to coordination polymer systems. The DFT-D method allowed us to fully optimize the lattice structures, even though the polymer chains interact only through dispersion forces. The optimized cell constants are $a = 8.76$ Å (−3.2%), $b = 7.52$ Å (+1.6%), $c = 5.20$ Å (−7.1%), $\beta = 101°$ $\beta$-$[Cu(pz)_2]_n$, **2**, and $a = 15.94$ Å (−6.0%), $b = 6.08$ Å (−2.6%), $c = 7.37$ Å (+1.3%) for $[Cu(pz)_2 \cdot (H_2O)]_n$, **3**. The underestimation of the lattice constants corresponding to the "soft" directions is similar to the one reported for DFT-D calculations on polyethilene.[8] In this work, the aims of the theoretical calculations are the following: (*i*) understanding the mechanism of the Cu(II)−Cu(II) antiferromagnetic coupling; (*ii*) evaluating the water-host bonding interaction; (*iii*) obtaining insight into the mechanism of pore formation by water sorption. Whereas the inclusion of dispersion forces was found to be unimportant for the determination of the electronic and magnetic properties, significant improvements were found in the estimate of the water sorption energy, and, most important, in the study of the energetics of the lattice transformation.

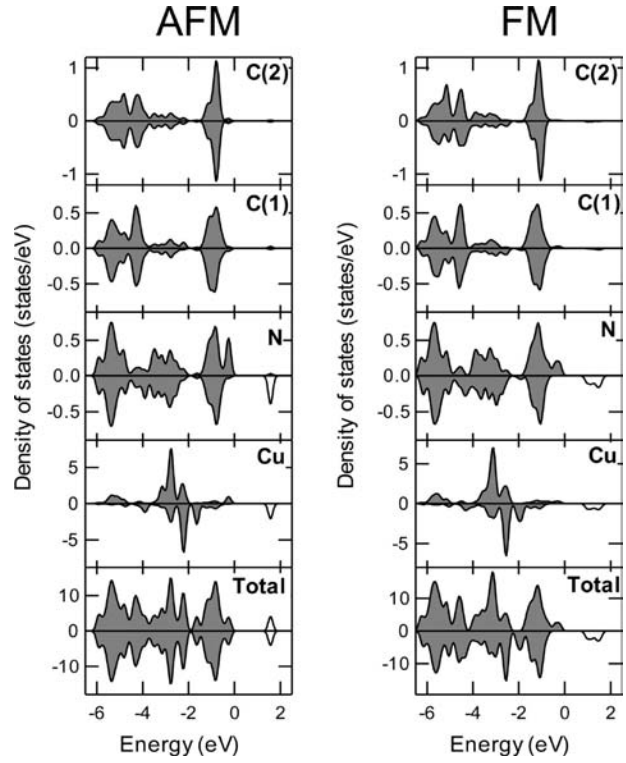


**Figure 5.** Spin-resolved density of states for $\beta$-$[Cu(pz)_2]_n$, **2**. Left: antiferromagnetic order; right: ferromagnetic order. Positive/negative values indicate spin up/down density of states. Filled areas indicate occupied states. Partial density of states are referred to single atoms. Atomic labels as indicated in Figure 1b.

We start from the analysis of the magnetic interactions in $\beta$-$[Cu(pz)_2]_n$, **2**. Both the FM and the AFM phases were found to be insulating, with a large band gap (see Figure 5), the AFM system being more stable by 0.051 eV/cell. The superexchange coupling constant $J$ can be evaluated from the total energies of the ferromagnetic, $E^{FM}$, and antiferromagnetic, $E^{AFM}$, phases through the formula:

$$E^{AFM} - E^{FM} = \frac{2zS^2J}{K} \qquad (3)$$

where the $z$ indicates the number of couplings per unit cell (2, in this case[23]), and $K = 8065.6$ is the conversion factor from eV to cm$^{-1}$. This allows us to estimate that $J = -415$ cm$^{-1}$. As found in similar calculations based on "pure" density functionals,[24] the coupling constant is significantly overestimated because of the excessively delocalized spin density.

More interesting is the information gained from local magnetic moments ($M$), which are obtained by projecting the wave functions into atomic functions (see Table 1), and from spin density maps (see Figure 6). As it clearly appears

(22) (a) Abragam, A.; Bleaney, B. *Electron Paramagnetic Resonance of Transition Ions*; Clarendon Press: Oxford, 1970. (b) Bencini, A.; Gatteschi, D. *Electron Paramagnetic Resonance of Exchange Coupled Systems*; Springer-Verlag: Berlin, 1990.

(23) In the case of $[Cu(pz)_2 \cdot H_2O]_n$ the factor 2 should be replaced by a factor 4 to account for the presence of 4 chain interactions in the unit cell (see Figure 1c).

(24) (a) Ruiz, E.; Llunell, M.; Alemany, P. *J. Solid State Chem.* **2003**, *176*, 400. (b) Doll, K.; Wolter, A. U. B.; Klauss, H.-H. *Phys Rev. B* **2007**, *75*, 184433.

**Table 1.** Local Magnetic Moments ($\mu_B$) Computed for Anhydrous and Hydrated Polymers in the AFM and FM States[a]

| | $\beta$-$[Cu(pz)_2]_n$, **2** | | $[Cu(pz)_2\cdot(H_2O)]_n$, **3** | |
|---|---|---|---|---|
| | AFM | FM | AFM | FM |
| Cu/Cu′ | 0.556/−0.556 | 0.574 | 0.573/−0.573 | 0.590 |
| N/N′ | 0.090/−0.090 | 0.098 | 0.092/−0.092 | 0.096 |
| C(1)/C′(1) | −0.005/0.005 | −0.002 | −0.006/0.006 | −0.002 |
| C(2) | 0.000 | 0.007 | 0.000 | 0.006 |
| O | | | 0.000/0.000 | −0.001 |

[a] Atoms are labeled as in Figure 1b.

from Figure 6, the Cu magnetic orbital is the d($x^2-y^2$) one, while the superexchange interaction is mediated by the $\sigma$ pyrazolate system. The spin density is largely carried by Cu and N atoms, only minor fractions of it being localized at the C(1) and C(2) sites (see Table 1). Local magnetic moments at the Cu ions are similar to those previously computed for other antiferromagnetic Cu polymers, Cu(thiazole)$_2X_2$, X =Cl, Br.[25]

Turning now to $[Cu(pz)_2\cdot(H_2O)]_n$, **3**, we first want to focus on the polymer-sorbate interaction. The equilibrium positions of water molecules were determined by performing several optimization runs, each started from different initial molecule orientations. In the most stable configuration, water molecules are oriented with the H atoms pointing toward the closest pyrazolate rings, as shown in Figure 7.

Optimized distances (in Å) are 0.98 (O−H); 2.85 (Cu···O); 3.34 ($\pi$···O); and bond angles (in degrees) are 104.3 (H−O−H); 80.7 (Cu−O−Cu). The computed Cu−O distances fairly agree with the experiment (ca. 2.91 Å) and are rather long even for a weakly bound species as a $\mu$-$H_2O$, being the usual Cu−O distance for a water molecule bridging Cu(II) ions below 2.4 Å.[26] This may be indicative that another species is competing in the interaction with the water molecules, as it occurs, for a lesser amount, for example, in the binuclear complex $\mu$-acetato- $\mu$-aqua- $\mu$-hydroxo-bis[(1,4-dimethyl-1,4,7-triazacyclononane-$\kappa$ *N*-3)-copper(II)] diperchlorate, where the electrostatic interaction between the $\mu$-aquo ligand and the counteranions lengthens the Cu−$OH_2$ distance to 2.737 Å.[27] In the present case, the competing interaction may be the O−H···$\pi$ one, occurring between the water hydrogens and the pyrazolate rings of the nearest polymer chain. Interestingly, the computed O···$\pi$ distance is typical for OH···$\pi$ interactions for phenyl rings in neutral organometallic compounds.[28] Because, in contrast to that, the Cu−$OH_2$ bonds are unusually elongated, we infer that the water-pyrazolate interaction is stronger than, or at least comparable to, the water-copper(II) one. This interpretation is supported by the electron difference density plots reported in Figure 8, which are obtained by computing the difference between the electron density of the *interacting* polymer−water system and that of a *non-interacting* system. The latter is obtained by summing the electron densities of the separated polymer and water moieties, each taken with the structure it assumes in the *interacting* system (i.e., the atomic positions are the same in both systems). These maps are useful to pinpoint the electron density rearrangements due to the formation of bonds and are particularly effective when dealing with molecular fragments. Looking at Figure 8, we can easily appreciate a considerable charge rearrangement in the Cu−O direction which is typical of weak electrostatic interactions:[29] the oxygen lone pairs are polarized toward the positive charged Cu atoms (see Figure 8b). In complete agreement with the previous discussion based on the simple inspection of interactomic distances, a *similar* and *comparable* charge rearrangement also occurs along the H···C directions (see Figure 8a). This similarity stems from the fact that also O−H···$\pi$ interactions are electrostatic in nature. On the other hand, the comparability of the charge rearrangements further confirms that the water-pyrazolate interactions are at least as strong as the water−Cu ones. Inter alia, this computational evidence may allow the comprehension of the "phase change" of **2** during water absorption (from a monoclinic to a orthorhombic lattice), likely driven by the formation of many (cooperative) OH···$\pi$ interactions in the lattice of **3**.

As far as the sorption energy is concerned, this can be straightforwardly computed from the total energies through the formula:

$$E_{sorpt}(H_2O) = E\{[Cu(pz)_2(H_2O)]\} - E\{\beta\text{-}[Cu(pz)_2]\} - E\{H_2O\}$$

while the water/host interaction energy ($E_{int}$) can be computed by using an analogous formula where the $\beta$-$[Cu(pz)_2]$ phase is replaced by an hypothetical relaxed "waterless" $[Cu(pz)_2\cdot(H_2O)]$ phase. The low (0.56 eV, 54 kJ/mol) computed $E_{sorpt}$ value explains the facile dehydration of the compound, while the $E_{int}$ value (0.71 eV, 69 kJ/mol) is well in tune with the electrostatic nature of the water-polymer interaction discussed above. Finally, magnetic moments (see Table 1) are scarcely affected by water sorption. Even lower is the effect on the relative energy of the FM and AFM phases (computed to be 0.050 eV/cell in favor of the latter), and, consequently, on $J$ (computed to be $-404$ cm$^{-1}$).

We now turn our attention to the mechanism of the structural rearrangement occurring during the water sorption/desorption process. As pointed out in the Introduction, the $\beta$-$[Cu(pz)_2]_n$, **2**, → $[Cu(pz)_2\cdot(H_2O)]_n$, **3**, transformation (as well as $[Cu(pz)_2\cdot(NH_3)]_n$, **1** → $\beta$-$[Cu(pz)_2]_n$, **2**) is characterized by reversibility and easiness. Because a first-principle simulation of the transformation is obviously not feasible,

(25) Zhou, L.; Yao, K. L.; Liu, Z. L. *J. Phys.: Condens. Matter* **2006**, *18*, 3325.

(26) (a) Chaudhuri, P.; Ventur, D.; Wieghardt, K.; Peters, E.-M.; Peters, K.; Simon, A. *Angew. Chem., Int. Ed. Engl.* **1985**, *24*, 57. (b) Christou, G.; Perples, S. P.; Libby, E.; Folting, K.; Huffman, J. C.; Webb, R.; Hendrickson, D. N. *Inorg. Chem.* **1990**, *29*, 3657. (c) Youngme, S.; van Albada, G. A.; Roubeau, O.; Pakawatchai, C.; Chaichit, N.; Reedijk, J. *Inorg. Chim. Acta* **2003**, *342*, 48. (d) He, H.-Y.; Zhou, Y.-L.; Zhu, L.-G. *Acta Crystallogr. C* **2004**, *60*, m569. (e) Barquin, M.; Gonzalez Garmendia, M. J.; Larrinaga, L.; Pinilla, E.; Torres, M. R. Z. *Anorg. Allg. Chem.* **2005**, *631*, 2151. (f) Gautier-Luneau, I.; Phanon, D.; Duboc, C.; Luneau, D.; Pierre, J.-L. *Dalton Trans.* **2005**, 3795. (g) Chailuecha, C.; Youngme, S.; Pakawatchai, C.; Chaichit, N.; van Albada, G. A.; Reedijk, J. *Inorg. Chim. Acta* **2006**, *359*, 4168.

(27) Elliot, D. J.; Martin, L. L.; Taylor, M. R. *Acta Crystallogr. C* **1998**, *54*, 1259.

(28) Braga, D.; Grepioni, F.; Tedesco, E. *Organometallics* **1998**, *17*, 2669.

(29) Casarin, M.; Maccato, C.; Vittadini, A. *J. Phys. Chem. B* **1998**, *102*, 10745.

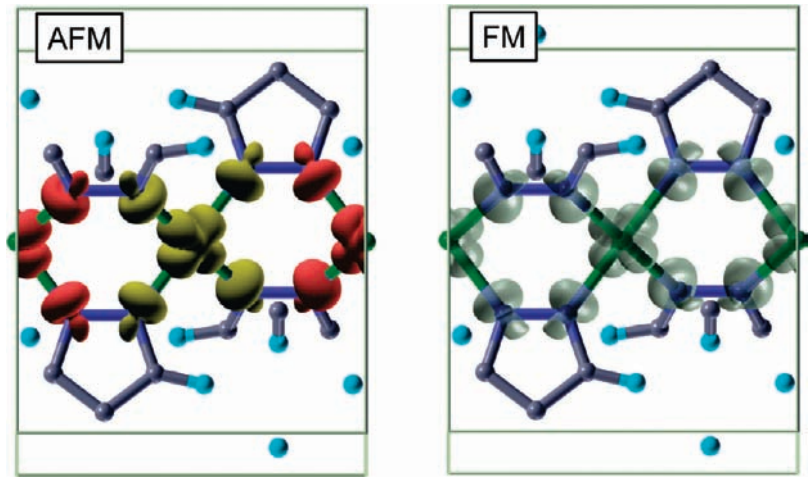


**Figure 6.** Three dimensional spin density maps for the AFM- (left) and the FM- (right) ordered phases $\beta$-$[Cu(pz)_2]_n$, **2** polymers. Displayed isosurfaces are $\pm$ 0.005 e/$a_0^3$. For the AFM order, yellow/red color surfaces have been used to show regions with positive/negative spin density. For the FM phase, where negative spin density is negligible, a semitransparent surface has been adopted.

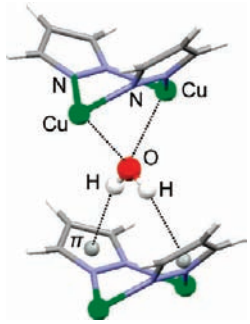


**Figure 7.** Local coordination of a water molecule to fragments of the nearest polymer chains in the AFM phase. Centroids of pyrazolate rings are displayed as gray balls and are marked by the $\pi$ symbol.

we focus on an idealized model process where only the rearrangement of the host structure is considered, as described in the following. In Figure 9, where **2** and **3** are viewed down the (010) and the (001) planes, respectively, the close metric relationship between the two structures is evident. If we now consider for **3** the smaller oblique cell (indicated by the solid lines) instead of the more symmetric rectangular one, it turns out that the **2** $\rightarrow$ **3** transformation can be approximately described as a lowering of the monoclinic $\beta$ angle from $\sim$100° (the value of the anhydrous $\beta$ phase) to $\sim$70° (the angle corresponding to the hydrated phase). This can be easily done by shifting, in the horizontal direction, adjacent rows of 1D chains, and passing from a dense structure to a porous one, favored by new OH$\cdots\pi$ interactions with the guest molecules. Accordingly, this structure modification is somehow triggered by water molecules initially adsorbed at the surface of the polymer, and finds its driving force in the water sorption enthalpy. Considering that the latter has been computed to be rather small, the energy barrier for changing the polymer structure is probably low. To estimate this barrier, we performed "linear transit" (LT) calculations where the $\beta$ parameter of the monoclinic structure of **2** was progressively lowered from 105° to 65° in 5° steps. Given the idealized nature of the investigated transformation, and the approximate nature of the LT approach, we avoided time-consuming variable cell calculations carrying out *two* sets of runs, where the cell constants were kept fixed at the theoretical values of **2** and **3**, respectively (see Figure 10).

The total energy curve obtained for the denser structures corresponding to the $\beta$-$[Cu(pz)_2]_n$ constants (Figure 10, squares) is characterized by a single, deep minimum at $\beta \sim 100°$, characteristic of the dehydrated compound, and by an inflection point at $\beta \sim 85°$. In contrast to that, two almost equivalent minima are found for the host structure when the constants of the more expanded $[Cu(pz)_2 \cdot (H_2O)]_n$ phase are taken. The second minimum is found at $\beta \sim 75°$, which is quite close to the value of the monoclinic cell of $[Cu(pz)_2 \cdot (H_2O)]_n$ phase. An estimate of the activation energy involved in the pore opening transformation (100° $\rightarrow$ 75°) is given by the energy of the crossing point between the two curves. The low resulting value (18 kJ/mol) explains the easiness of the water sorption process. On the other hand, the almost vanishing barrier for the backward (75° $\rightarrow$100°) transformation indicates that the solvent-free porous structure is unlikely to be obtained. Overall, our approximated potential energy curve is quite well compatible with the reversibility of the water absorption/desorption process.

## Conclusions

Solid microcrystalline coordination polymer $\beta$-$[Cu(pz)_2]_n$, **2**, can adsorb, reversibly, one molecule of water generating the hydrated species $[Cu(pz)_2 \cdot (H_2O)]_n$, **3**. In this solid state process, the monoclinic structure of **2** changes to the orthorhombic **3** and, being that the structure of **2** is compact, without pores or channels, water accommodates in voids that are "generated" in the adsorption process, a particular case of porosity "without pores".[1] In the present paper we report, besides a new, more profitable synthetic procedure to obtain **2**, an experimental and theoretical study on the magnetic properties of **2** and of the hydrated phase **3**, carried out by magnetic susceptibility measurements, EPR spectroscopy, and DFT-D calculations.

Both theoretical and experimental evidence show that Cu(II) ions are antiferromagnetically coupled with a relatively strong exchange interaction. The additional water molecule in the hydrated phase slightly increases the interaction between copper ions. Inspection of the theoretical spin

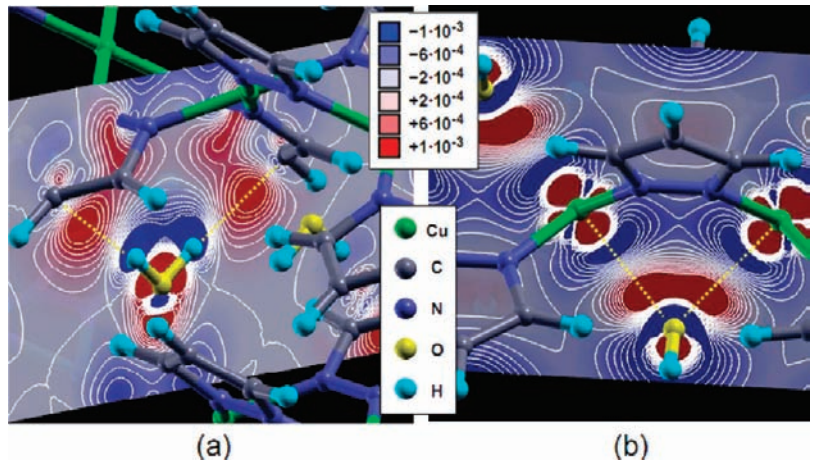


**Figure 8.** Electron difference density plots referring to the $H_2O-Cu(pz)_2$ interaction (see text). Displayed sections are as follows: (a) a (100) plane bisecting two pyrazolate rings which bridge the same Cu atoms; (b) a (001) plane passing through the Cu atoms of a polymer chain.

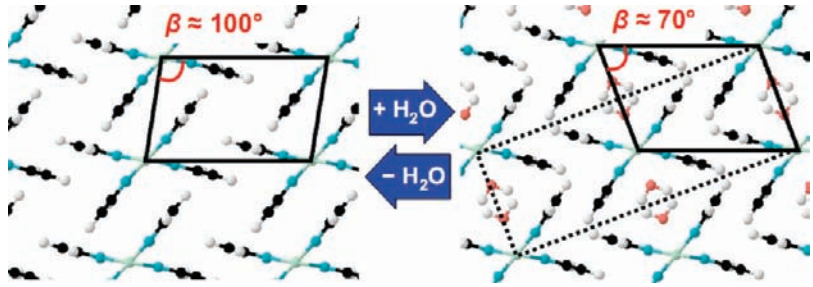


**Figure 9.** Left: view of the lattice structures of $\beta$-$[Cu(pz)_2]_n$, **2**, down the (010) plane. Right: view of the lattice structure of $[Cu(pz)_2 \cdot (H_2O)]_n$, **3**, down the (001) plane. Solid lines show the monoclinic cells. The dashed line on the $[Cu(pz)_2 \cdot (H_2O)]_n$, **3** structure indicates the orthorhombic cell.

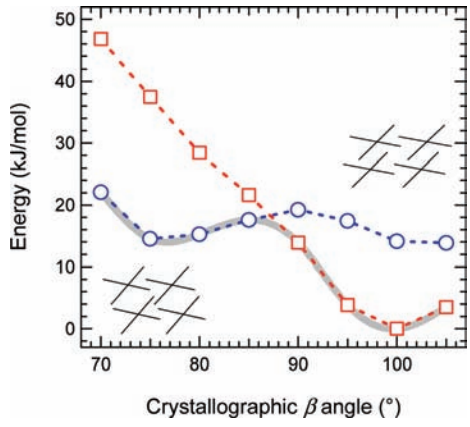


**Figure 10.** Total energy curves obtained by scanning the monoclinic $\beta$ angle of the dehydrated phase over a 5°-spaced grid. The cell edges are kept fixed at the theoretical values corresponding to $\beta$-$[Cu(pz)_2]_n$, **2** (squares) and to $[Cu(pz)_2 \cdot (H_2O)]_n$, **3**, (circles) experimental structures. Energies are referred to 1 mol of $Cu(pz)_2$. The gray curve indicates the (approximate) path followed by the lattice transformation, schematically shown in the insets.

densities show that the dominant magnetic interactions involve the $\sigma$ orbitals of the pyrazolate ligands. Furthermore, calculations show that the long $H_2O-Cu(II)$ distances are due to the concurrent interaction between the water protons and the pyrazolate rings of the neighboring chains. The energetics of the pore opening mechanism has also been studied, finding that the energy barriers for the pore formation are indeed low.

**Acknowledgment.** This work was supported by the Italian PRIN (n. 2006038447) and by FIRB 2003 (n. RBNE033KMA) funds. Computational resources and assistance were provided by the Laboratorio Interdipartimentale di Chimica Computazionale (LICC) at the Department of Chemistry of the University of Padova. Density functional calculations have been performed by using the Quantum-ESPRESSO package.[9] Molecular graphics have been generated by XcrysDen[30] and Mercury.[31]

IC801928B

(30) Kokalj, A. *Comput. Mater. Sci.* **2003**, *28*, 155; Code available from http://www.xcrysden.org/.
(31) Bruno, I. J.; Cole, J. C.; Edgington, P. R.; Kessler, M.; Macrae, C. F.; McCabe, P.; Pearson, J.; Taylor, R. *Acta Crystallogr. B* **2002**, *58*, 389; Available from http://www.ccdc.cam.ac.uk.